Analysis of the hypernetted chain equation for ionic fluids

Johan S. Høye

Institutt for Fysikk, Universitetet i Trondheim,
N-7034 Trondheim-NTH, Norway

Enrique Lomba[†]

Department of Chemistry, State University of New York
at Stony Brook, Stony Brook, NY 11794-3400, USA

George Stell

Departments of Chemistry and Mechanical Engineering, State University of New York
at Stony Brook, Stony Brook, NY 11794-3400, USA

It is well known that the numerical solution of the hypernetted chain equation (HNC) yields satisfactory results for the pair correlation function of the primitive model of electrolytes and similar models of ionic particles over a considerable range of thermodynamic states. Despite this, it has become apparent that for low densities (or low ionic concentration in electrolytes) the numerical solution breaks down for temperatures well above the expected coexistence region between gas and liquid phases. Here we study situation by analytic means, comparing it to a similar problem for sticky hard spheres in the Percus-Yevick (PY) approximation. On the basis of our analysis we conclude that the failure of the HNC is of the same nature and is connected to the existence of two possible solutions for low densities. When the temperature is lowered these solutions will merge into one at a particular temperature, below which a real solution is no longer possible. By extending our analysis to systems like the monoatomic Lennard-Jones fluid and comparing with previous results of Gallerani, Lo Vecchio and Reatto for two-Yukawa and Lennard-Jones systems in the PY approximation, we conclude that these are general common features of the HNC and PY approximations in the low-density regime. Numerically they appear to *well* persist in the HNC approximation at high densities as (in contrast to the behavior of the PY approximation) although our analysis is silent in this regard. Our analysis is consistent with the results of a recent comprehensive numerical study by Belloni.

[†]Permanent address: Instituto de Química Física Rocasolano, CSIC, Serrano 119, E-28006 Madrid, and Depto. Química Física I, U. Complutense, E-28040 Madrid, Spain

I. INTRODUCTION

Strong evidence has accumulated that at low densities the numerical solution of the Ornstein-Zernike (OZ) equation with hypernetted-chain (HNC) closure breaks down badly when applied to ionic fluid models such as the restricted primitive model (RPM). In an earlier study,[1] referred to as I hereafter, we probed these numerical difficulties for an ionic fluid to gain insight into the nature of the singularity responsible for the resulting low-density boundary of the HNC "no solution" region. Although numerical inaccuracy makes it hard to delineate this region with high accuracy, the region is certainly not a numerical artifact. Here we give an analytic description of the region that we have formulated.

Although for liquid densities isothermal compressibilities appear to diverge in the vicinity of the no-solution region, as was seen in I, very recent work by Belloni[2] has shown that in fact their value remains finite for all densities, in accordance with partial results previously obtained by Kinoshita and Harada.[3] Indeed, a re-analysis of our previous results for high density carried out in Section IV herein also shows that the lack of spinodal behavior on the low-density side appears to extend to the high-density branch too. One does not appear to have spinodal behavior on either the high-density or low-density sides of the no-solution line, but rather some of the typical features of a coexistence curve, and it is tempting to identify the no-solution line as the approximation's way of generating such a curve. Unfortunately its location is very far from the best estimates of where the RPM coexistence curve can be expected to lie.

In the above discussion (and throughout the rest of this paper) when we refer to compressibility we mean the isothermal compressibility computed via the fluctuation integral that relates the inverse compressibility to an integral over a direct correlation function. By spinodal line we mean the locus of points on which the compressibility is infinite. In the HNC approximation, the thermodynamics computed via the virial theorem or via the internal-energy integral over a radial distribution function times a pair potential will not be consistent with this compressibility (but will be consistent with each other). In the HNC approximation, it is only the thermodynamics computed via the fluctuation integral that is directly connected to the range of the density-density pair correlation function.

In Ref. 1 we noted that the present problem might have some features similar to the sticky-sphere problem solved by Baxter with Percus-Yevick boundary conditions.[4] Cummings and Stell analyzed this solution in comparison with the mean spherical approximation (MSA) for a Yukawa interaction, which also can be solved analytically.[5] According to their analysis and numerical evaluations, the MSA Yukawa problem has a unique physically acceptable solution as the temperature is lowered for fixed density until the spinodal line is reached. Beyond this line the continuation of the physically acceptable solution and a second real solution merge when a second line is reached. Beyond this second line the two solutions become complex.

In the PY solution for a system of sticky hard spheres there is similar behavior at

liquid densities. However, for low densities it turns out that there will be a crossover at a critical point such that below the critical density, the physically acceptable solution and a second real solution will merge to become complex <u>before</u> the spinodal line is reached, as one lowers the temperature. The result is a no-solution locus in the $\rho - T$ plane that is not a spinodal line below the critical density ρ_c but is instead a line associated with finite compressibility, that shares many of the features of the low-density branch of a coexistence curve.

Our conclusion is that the behavior of the HNC approximation for ionic systems such as the RPM is of a similar nature and can then be related to the same mechanism that one finds at low density for sticky hard spheres in the PY approximation. This conclusion is motivated by the observation that oppositely changed ions in the HNC approximation behave much like sticky hard spheres in the PY approximation immediately outside the hard cores of the pair potentials, giving rise to narrow sharply peaked contributions to the distribution functions that have a similar thermodynamic effect in the two cases. The argument can be made precise in a mathematical development given in Section III.

II. STRUCTURE OF THE ORNSTEIN-ZERNIKE EQUATION

A. Remarks in the context of the MSA

To better understand qualitatively the properties of the HNC approximation one can profit from first analyzing the simpler MSA and PY sticky-sphere cases. All these theories are based on solutions of the OZ equation for hard-core potentials. Their difference lies in the way the direct correlation function $c(r)$ is approximated outside the core. For the MSA the direct correlation function outside the core is given by $-\beta\phi(r)$ where $\phi(r)$ is the interaction potential, and $\beta = 1/kT$, $k =$ Boltzmann's constant and $T =$ temperature. Now the HNC and PY sticky-sphere equations can be regarded as effective MSA problems too, but with effective $\phi(r)$ that are density and temperature dependent functions, defined by $c(r) = -\beta\phi^{eff}(r)$.

We first consider the MSA one-component case with Yukawa interaction. This has already been solved analytically and analyzed.[6-8] The algebraic equations for this latter problem have several solutions of which only one is physically acceptable for a given temperature and density. In the present instance physical acceptability is associated with a correlation function that decays with distance and is real. (In a different context we also have dealt with complex MSA correlation functions to represent propagation of electromagnetic waves in dielectric media at non-zero frequency.[9,10])

Now the physically acceptable solution is accompanied by a neighboring unphysical solution, and if one plots the inverse compressibility associated with each solution as a function of inverse temperature one gets two curves, with the acceptable one going to its minimum at zero (spinodal curve), and then continuing as a non-acceptable solution which will merge with the other neighboring solution, at which point the pair of solutions become complex as one further lowers the temperature.

3

The property of having a pair of solutions that merge in a parameter space can be expected to be a general property that follows from the structure of the OZ equation and is not limited to a potential of Yukawa form. This property will also persist for approximations other than the MSA. For these other approximations the two solutions in question will, when interpreted in the context of the MSA, represent two somewhat different interactions. As a rough approximation these two interactions can be regarded as having the same form, *e.g.* a Yukawa form. What is important is that the two solutions will then represent two different MSA temperatures, and again they will merge when the true temperature of the system at hand is lowered. However, the point of merging will be shifted along the curve of solutions and can in principle be anywhere depending upon the relation between the pair of MSA temperatures. In particular it is possible for this point to lie in a region of thermodynamic stability. Thus by lowering the temperature when performing a numerical solution in such a region of thermodynamic stability this point will be reached without passing through a spinodal curve. When they meet, a change of input parameters will no longer give a real solution. Thus the numerical procedure will fail. (As an illustration one could solve the MSA for fixed inverse compressibility. The two solutions will meet precisely at the spinodal curve since the curve of solutions has zero as minimum inverse compressibility.)

B. PY solution for sticky hard spheres

The merging of two solutions in the physically acceptable region as described above can be easily demonstrated in an analytic way by considering sticky hard spheres with PY boundary condition. This problem has been solved by Baxter[4] and its solution has been investigated by Cummings and Stell[5] and they find that two solutions merge in the physically acceptable region for low densities. We reinvestigate this situation in language appropriate to our study and reestablish some results. The PY condition connecting the pair function $h(r)$ and direct correlation function $c(r)$ is

$$(1 + h(r)) f(r) = c(r) (1 + f(r)) \tag{1}$$

where

$$f(r) = e^{-\beta\phi(r)} - 1$$

is the Mayer function. Eq.(1) can be rewritten as

$$c(r) = f(r)y(r), \tag{2}$$
$$y(r) = 1 + h(r) - c(r)$$

where $(1 + f(r))y(r) = 1 + h(r)$ defines $y(r)$. For sticky spheres $f(r)$ is -1 inside the hard cores and is a δ-function on the hard-core surface. This δ-function can now be represented by a term of Yukawa form. Following Ref. 4, we can write

4

$$1 + f(r) = \begin{cases} 0 & \text{if } r < 1 \\ \frac{1}{12\tau}\delta(r-1) + 1 & \text{if } r \geq 1 \end{cases} \tag{3}$$

From the structure of the OZ equation $h - c$ will be a smooth function at $r = 1$ in which the δ-function will not appear. Eq.(2) implies that $c(r) = 0$ outside the δ-function and that $y(r)$ is also smooth at $r = 1$. Accordingly at the hard core we can write

$$h(r) = \frac{1}{12}\lambda_1\delta(r-1) \quad \text{at} \quad r = 1 \tag{4}$$

and also

$$c(r) = \frac{1}{12}\lambda_1\delta(r-1) \rightarrow Ke^{-z(r-1)}/r \quad \text{for } r \geq 1 \tag{5}$$

with $z \rightarrow \infty$ ($\frac{1}{12}\lambda_1 = K/z$). From Eqs.(2)-(4) λ_1 is given by

$$\lambda_1 = y(1)\frac{1}{\tau} \tag{6}$$

With condition (5) on $c(r)$ we are back to the MSA Yukawa problem with unique physically acceptable solution for given K and λ_1. However, with PY sticky spheres τ is the given parameter related to λ_1 via Eq.(6). To obtain explicit results, $y(1)$ is needed. This quantity is found in the Appendix by means of Baxter's factorization method . The result is

$$y(1) = \frac{1 + \xi/2}{(1-\xi)^2} - \frac{\xi\lambda_1}{1-\xi} + \frac{1}{12}\xi\lambda_1^2 \tag{7}$$

Inserted in (6) this yields precisely the equation analyzed in Ref. 5 based upon the solution found in Ref. 4. The inverse compressibility becomes

$$a_0 = 1 - \rho\tilde{c}(0) = \left(1 - 12\xi\tilde{Q}(0)\right)^2 = a^2 = \left[\frac{1 + 2\xi - \xi(1-\xi)\lambda_1}{(1-\xi)^2}\right]^2 \tag{8}$$

In Eqs.(7) and (8) the $\xi = \frac{\pi}{6}\rho$ is the packing fraction for spheres of unit diameter, and ρ is the number density. It may be noted that the neighboring solution of (8) is missing here. This is because the limit $z \rightarrow \infty$ (see Eq.(5)) is taken, whereby $a_0 \rightarrow \infty$ for this latter solution. In this limit the two solutions will not merge for finite λ_1 either. However, the spinodal curve $a_0 = 0$ will be present at which

$$\lambda_1 = \lambda_s = \frac{1 + 2\xi}{\xi(1-\xi)} \tag{9}$$

5

Thus only values of λ_1 smaller than λ_s will be physically acceptable, and larger values of λ_1 can be considered as the finite part of the other solution.

Solution of Eq.(7) when inserted in (6) yields two values of λ_1 for given τ. For small $1/\tau$ there will be an acceptable solution $\lambda_1 < \lambda_s$ and an unacceptable one $\lambda_1 > \lambda_s$. However, when $1/\tau$ increases these solutions will approach each other and they will finally merge. For large ξ it is then found they they merge for $\lambda_1 = \lambda_m > \lambda_s$, but for small ξ they merge for $\lambda_1 = \lambda_m < \lambda_s$, i.e. in the physically acceptable region. This has the important consequence that the spinodal curve $a_0 = 0$ can not be reached by increasing $1/\tau$ as solutions will become complex beyond the point at which $\lambda_1 = \lambda_m$.

The solutions merge when the square root they contain becomes zero. Then the common solution will be

$$\lambda_1 = \lambda_m = \frac{6}{\xi}\left(\frac{\xi}{1-\xi}+\tau\right) = \frac{[6\xi(2+\xi)]^{1/2}}{\xi(1-\xi)} \tag{10}$$

This coincides with $a_0 = 0$ when $\lambda_m = \lambda_s$, i.e. for

$$\xi = \xi_c = -2 + \sqrt{4.5} = 0.1213 \tag{11}$$

as found in Ref. 5.

We note that the curves for λ_s and λ_m cross at the compressibility critical point: i.e. this point is the one that corresponds to the largest value of τ along the spinodal curve, and at the same time yields the largest value for which the two solutions merge. (See Fig. 1 of Ref. 5.) At the latter maximum the relation (10) between τ and ξ has to be fulfilled. In addition the derivative of τ with respect to ξ is zero at this point, since τ reaches a maximum. Differentiation of Eq.(10) with a factor $6/(\xi(1-\xi))$ first taken out for convenience then yields

$$1-\tau = \frac{1+\xi}{[6\xi(2+\xi)]^{1/2}} \tag{12}$$

When solved with respect to ξ this, together with (10), yields the same point as the critical point defined by Eq. (11).

III. HNC FOR THE RPM AT LOW DENSITIES

The above analysis made for PY sticky spheres is relevant for the HNC for ionic fluids. The reason is that ions at temperatures corresponding to their gas-liquid critical point will act much like sticky spheres when ions of opposite charges meet due to the strong Coulomb forces immediately outside the hard cores, if one neglects the extended long range of the Coulomb interactions.

Furthermore for sufficiently low densities we show below that PY and HNC boundary conditions are equivalent for sticky spheres. Thus the RPM in the HNC approximation and sticky spheres in the PY approximation can be closely identified with

6

each other, *i.e.* they can be expected to have common properties. One such property will be the merging of solutions before the spinodal line is reached for low densities. For the HNC ionic fluid case, however, the merging of solutions appears to occur for all densities, as Belloni has found recently on the basis of an extremely accurate numerical analysis.[2] From the results in the preceding section we estimate where the solutions should meet and compare with previous numerical results for the breakdown of the HNC solution for the primitive electrolyte.

The HNC closure when restricted to a one component system for simplicity, reads

$$c(r) = \exp\left(-\beta\phi(r) + \gamma(r)\right) - 1 - \gamma(r) = (1 + f(r))\, e^{\gamma(r)} - 1 - \gamma(r) \qquad (13)$$

with $\gamma(r) = h(r) - c(r)$. The PY condition (1) can be written

$$c(r) = f(r)\, (1 + \gamma(r)) \qquad (14)$$

Expansion of Eq.(13) yields

$$c = (1 + f)\left(1 + \gamma + \frac{1}{2}\gamma^2 + \dots\right) - 1 - \gamma \qquad (15)$$

$$= f\, (1 + \gamma) + (1 + f)\left(\frac{1}{2}\gamma^2 + \dots\right)$$

Besides being a smooth function the $\gamma(r)$ will also vanish along with density. Thus the last term of Eq.(15) can be neglected, and the HNC condition becomes the PY condition. Thus as an approximation we can apply Eqs.(6) and (7) to ionic fluids. The failure of numerical solution, *i.e.* the merging of solutions, should occur at the value of τ implied by Eq. (10). For small ξ this becomes

$$\tau = \sqrt{\frac{\xi}{3}} \qquad (16)$$

The τ can further be expressed in terms of the stickiness of the attractive Coulomb interaction

$$\phi = -\frac{e^2}{r} \qquad (17)$$

Expanding with $r = 1 + u$ we get

$$1 + f(r) = e^{-\beta\phi(r)} = e^{\beta^*(1 - u + \dots)}$$
$$\approx \beta^{*-1} e^{\beta^*} \delta(r - 1) \qquad (18)$$

with $\beta^* = \beta e^2$. Comparison with Eq. (3) then gives τ, which inserted in Eq.(16) yields the curve where the solutions merge given by

$$\xi = \frac{1}{48}\beta^{*2} e^{-2\beta^*} \qquad (19)$$

7

This analysis can also be applied if ions interact through shielded potentials of the form

$$\phi(r) = e^2 \frac{\exp(-zr)}{r} \qquad (20)$$

which appears in the restricted primitive Yukawa model (RPYM).[16] In this case, we find the following relation

$$\xi = \frac{1}{48(1+z)^2} \beta^{*\prime 2} e^{-2\beta^{*\prime}} \qquad (21)$$

with $\beta^{*\prime} = \beta^* e^{-z}$. In Fig. 1 these curves have been plotted along with numerical results for the Coulomb fluid ($z = 0$) and shielded RPM with $z = 1$ and $z = 2$. These analytic but approximate predictions can be seen to yield quite accurate the limiting slopes of the curve for low ξ. With increasing shielding, a careful numerical analysis shows that the relative separation between the analytical estimates and the numerical non-solution loci shrinks since the range of the potential diminishes, and the properties of the model thereby approach those of a sticky sphere system. One would not expect its properties to approach those of the Baxter one-species sticky sphere model, however, but rather those of a binary-mixture model with stickiness only between unlike species which are held at equal density. Similarly because the above mathematics was done in the context of a one-species model, our conclusions must be qualified somewhat when applied to the RPM or RPYM, which are binary-mixture models. For such models, the correlations that directly determine compressibility are the density-density correlations or "sum" functions $h_S(r) = [h_{++}(r) + h_{+-}(r)]/2$ and $c_S(r) = [c_{++}(r) + c_{+-}(r)]/2$, which obey their own Orstein-Zernike equation. But for the RPM or RPYM, the Coulomb or Yukawa potentials, respectively, do not appear as the dominant contribution to $c_S(r)$ since $[\phi_{++}(r) + \phi_{+-}(r)]/2 = 0$ for such $\phi_{\alpha\beta}(r)$. Instead one thinks of $h_S(r)$ and $c_S(r)$ as describing a hypothetical one-component system, then the effective $\phi(r)$ in that system is shielded even in the Coulombic case, with a functional form and shielding parameter that are density and temperature dependent. It is this effective $\phi(r)$ that has to be used to the analysis rather than the $\phi(r)$ of (17) or (20) if a more quantitatively accurate result is desired. Unfortunately, such an analysis can no longer be made in a simple closed form. However, to a good approximation, the result is that using a $\phi(r)$ of the form given by (20) for both the RPM and RPYM, with a renormalized e and z. In both cases the only substantial difference between the RPM and RPYM cases comes from the fact that the effective RPM $\phi(r)$ loses its shielding as $\rho \to 0$ (because as $\rho \to 0$, its shielding becomes simple Debye shielding) while the effective $\phi(r)$ for the RPYM will retain the shielding of the bare Yukawa potential even at zero density. It is this effect that appears largely responsible for the much greater asymmetry (in ρ) of the RPM no-solution curves compared to the RPYM curves that one finds numerically in the HNC approximation.

Our analysis, used with Eq. (20), applies directly as it stands to the single-species hard-core Yukawa fluid and is also obviously relevant to the two-Yukawa version of that model as well as the Lennard-Jones fluid. Our analysis therefore reveals a common feature of the no-solution line whenever that line is reached before the spinodal condition is satisfied. This feature is shared at low density by both the PY and HNC approximations and is common to both ionic and non-ionic models.

In our earlier HNC study, we found numerically that the compressibility was sufficiently high along the high-density side of the no-solution line to warrant the assumption that it became a spinodal beyond a certain crossover density, as it does in the PY case. Belloni's subsequent numerical results of extremely high precision[2] and our own further numerical analysis instead strongly support the conclusion that the spinodal is not reached for any accessible states. The good agreement we found in our earlier paper[1] between spinodal results for the structure factor and our numerical low-k structure factor results (close to the no-solution locus at $\rho = 0.5$) indicates that the spinodal approximation is nevertheless useful near and on the no-solution line at high densities, where the a/b^2 of Eq. 22 is large compared to unity. Thus we include our spinodal analysis as Section V.

IV. A NUMERICAL ANALYSIS OF SIMILARITIES WITH RELATED SYSTEMS: TWO-YUKAWA PY AND LENNARD-JONES PY AND HNC

One may ask to what extent one can go beyond the above discussion in relating the HNC results for the RPM to results for other equations and systems. In this regard we must first recall a previous work by Gallerani, Vecchio and Reatto[11] in which a careful study of the critical behavior of a two-Yukawa fluid in the PY approximation is presented and its further extension to PY Lennard-Jones.[12] In accordance with our findings and with results for the PY sticky hard-sphere fluid (both for continuum[4] and lattice-gas models[13]) Gallerani et al. show that there is a clear cut difference between the behavior of the system in the low- and high-density regions. Again as in the RPM, a no-solution line is reached at low densities before the spinodal. In contrast on the high density side they find that the no-solution curve is "hidden" by the spinodal divergence, i.e. the spinodal is reached as one lowers the temperature at a given density before the no-solution curve. Besides, Gallerani et al. propose an expression that describes the behavior of the isothermal compressibility along a isochore close to the no-solution line, namely

$$\chi_T(T,\rho) = \frac{a}{\left(b + \sqrt{T^* - T_n^*}\right)^2} \tag{22}$$

where a and b are parameters dependent on ρ and $T^* = 1/\beta^*$; T_n^* is the temperature at the no-solution line. Hence, the compressibility would remain finite at T_n^* exhibiting a square-root branch point. Since as shown by Eqs.(13) and (14) HNC and PY equations are closely related at low density, we have carried the analysis of Gallerani

9

et al. over to the RPM HNC and to a monoatomic Lennard-Jones fluid in the HNC approximation. Moreover, Belloni has shown[2] that in the HNC one must expect this type of behavior at liquid densities (or high concentrations in the RPM), *i.e.*, as mentioned before the no-solution line is reached before the spinodal for all densities investigated by Belloni. Note that Eq. (22) is in accordance with the divergence in the quantity $d\chi/d\Gamma$ depicted in Fig. 6 of I.

The adequacy of Eq.(22) to describe the isothermal compressibility behavior close to the no solution locus can readily be appreciated in Fig. 2, where this quantity is plotted *vs.* reduced temperature ($T^* = kT/\epsilon$ for the LJ system and $T^* = \Gamma = kT\sigma/e^2$ for the RPM). The lines represent a three-parameter non linear fitting of the integral equation results to Eq. (22) using the complex method.[17] Additional calculations which we omit for brevity, show that Eq.(22) is not only valid in the gas (low concentration) phase, but in contrast to what happens in the PY approximation[11] it extends to densities well above the critical, as was suggested by Belloni.[2] We note in passing that if one attempts to replace Eq. (22) by its spinodal counterpart (Eq.(7) in Ref. 12), which is valid for the PY-LJ system, the fitting is extremely poor. Finally in Fig. 3 we have plotted the density dependence of the b parameter in Eq. (22) which measures the deviation from true spinodal behavior. It can be seen that as density increases the no-solution line very likely tends to squeeze itself against a hidden spinodal, thus decreasing the value of b. It remains to be seen to which extent the high-density behavior of the HNC equation is shared by the RHNC approximation, for which Poll and Ashcroft[15] found a spinodal singularity, but without power law behavior. The RHNC approximation differs appreciably from the HNC at high densities because of the T^* and ρ-dependence of the reference system bridge function, which does not appear in the HNC analysis.

V. PROPERTIES OF THE HNC SOLUTION VERY NEAR THE SPINODAL

We shall now derive some results concerning the HNC correlation functions for ionic systems assuming that we are close enough to the spinodal so that $\chi_T^{-1} \ll 1$ and we can use the approximation $\chi_T^{-1} \approx 0$. (As mentioned in the preceding analysis, there is strong evidence that the condition $\chi_T^{-1} = 0$ is never realized in the HNC.) Our approach extends earlier work on non-ionic fluids by Green using the HNC equation[18] and by one of us (GS) with Lebowitz, Baer and Theumann using related approximations.[19]

Our results are based on the asymptotic (small-k, large-r) analysis of the solution of the HNC equation. For models of interest to us here, it is most convenient to do the analysis in terms of the correlation functions $h_S(r) = [h_{++}(r) + h_{+-}(r)]/2$ and $h_D = [h_{++}(r) - h_{+-}(r)]/2$ and the corresponding direct correlation functions $c_S(r) = [c_{++}(r) + c_{+-}(r)]/2$ and $c_D = [c_{++}(r) - c_{+-}(r)]/2$. The s and D functions describe the density-density and charge-charge correlations, respectively. In terms of the Fourier transforms $\tilde{h}_S(k)$ and $\tilde{c}_S(k)$ and the structure factor $S(k) = 1 + \rho\tilde{h}(k)$ ($\rho = \rho_+ + \rho_-$) the OZ equation for the S functions takes the form

10

$$S^{-1}(k) = 1 - \rho\tilde{c}(k) \tag{23}$$

where the HNC closure implies that for $r \to \infty$

$$c_S(r) = \frac{1}{2}\left[h_S^2 + h_D^2\right] + \text{ negligible terms} \tag{24}$$

Assuming that $S^{-1}(0) << 1$ so that we can use the spinodal condition $S^{-1}(0) = 0$, we find that on such a spinodal, a solution to the HNC equation will have the asymptotic form such that for large r and small k

$$h_S(r) \approx B/r^2, \quad \tilde{h}_S(k) \approx 2\pi^2 B/k \tag{25}$$
$$c_S(r) \approx B^2/2r^4, \quad \tilde{c}_S(k) \approx -\pi^2 B^2 k/2 \tag{26}$$

so that on the spinodal

$$S^{-1}(k) = Dk + O(k^2) \tag{27}$$
$$D = \rho\pi^2 B^2/2 \tag{28}$$

(Off the spinodal line this sharp linear behavior about $k = 0$ will be rounded off somewhat.) Moreover, using the OZ equation we can solve for B and D to find

$$B^3 = \pi^{-4}\rho^{-2}, \quad D = (2\pi^{2/3})^{-1}\rho^{-1/3} \tag{29}$$

Associated with this solution is a $h_D(r)$ that, unlike $h_S(r)$, is damped by an exponentially decaying factor as $r \to \infty$ and hence does not exhibit power law behavior in r.

It is of interest[20] to consider the effect of a cavity term added to the RPM pair potential $\phi_{++}(r), \phi_{+-}(r)$. This term has the form Ar^{-4} where

$$A = \frac{(\epsilon - 1)(z_+^2\sigma_{++}^3 + z_-^2\sigma_{--}^3)e^2}{16(2\epsilon + 1)\epsilon} \tag{30}$$

where ϵ is the dielectric constant of the solvent (relative to vacuum) and we shall consider the case of monovalent ions of unit diameter, $z_+^2 = z_-^2 = \sigma_{++} = \sigma_{--} = 1$.

In the presence of the cavity term, (24) becomes

$$c_S(r) = -\beta Ar^{-4} + \frac{1}{2}\left[h_S^2 + h_D^2\right] + \text{ negligible terms} \tag{31}$$

This changes the relations among the constants in the solution of the HNC equation. The introduction of A in (31) now yields a cubic equation for B

$$B^3 - 2\beta BA - B_0^3 = 0 \tag{32}$$

where $B_0^3 = \pi^{-4}\rho^{-2}$, the value of B^3 at $A = 0$.

ACKNOWLEDGMENTS

APPENDIX

To obtain Eqs. (7) and (8) we will use Baxter's factorization method which also has been used by Høye and Blum in Ref. 8. The Ornstein-Zernike equation can then be written as

$$rh(r) = -Q'(r) + 12\xi \int_0^\infty dt (r-t) h(|r-t|) Q(t) \tag{A1}$$

The function $Q(r)$ is zero for $r > R$, as is $c(r)$. (When $c(r)$ has terms of Yukawa form in this region the $Q(r)$ will have terms of exponential form.) Furthermore the connection to $\tilde{c}(k)$, which we will need here (for $k = 0$), is

$$1 - \rho \tilde{c}(k) = \tilde{Q}(k)\tilde{Q}(-k) \tag{A2}$$

with

$$\tilde{Q}(k) = 1 - 12\xi \int_0^R dr e^{ikr} Q(r)$$

In our case the Yukawa term in $c(r)$ shrinks to a δ-function at the hard-core surface, *i.e.* we have $R = 1$. Inspection of Eq. (A1) then requires $Q(r)$ to be of the form

$$Q(r) = \begin{cases} \frac{1}{2}ar^2 + br - (\frac{1}{2}a + b) + \lambda & r \le 1 \\ 0 & r > 1 \end{cases} \tag{A3}$$

Thus $Q(r)$ is a step function, whereby $Q'(r)$ becomes a δ-function ar $r = 1$. So with (A1) we have

$$h(r) = -1 + \lambda \delta(r-1) \quad r < 1^+ \tag{A4}$$

when the core condition also is included. Thus, comparing with Eqs. (4) and (5), we have

$$\lambda = \frac{1}{12}\lambda_1 \tag{A5}$$

12

We need the value of $h(r)$ just outside the δ-function. For this, (A1) yields

$$h(1^+) = 12\xi \int_0^1 dt(1-t)h(1^+ - t)Q(t) \tag{A6}$$

$$= -12\xi \int_0^1 dt(1-t)Q(t) + 12\xi\lambda Q(0)$$

Before simplifying this we establish the equations that determine a and b by using Eq. (A1) for $r < 1$. We get

$$-r = ar - b - 12\xi \int_0^1 dt \ (r-t)Q(t)$$

or

$$b = 12\xi \int_0^1 dt \ tQ(t) \tag{A7}$$

$$1 - a = 12\xi \int_0^1 dt \ Q(t)$$

With Eq. (A3) inserted this yields

$$(1 - 4\xi)a - 6\xi b = 1 - 12\xi\lambda \tag{A8}$$
$$-3\xi a - 2(1 + 2\xi)b = -12\xi\lambda$$

These equations give the solution

$$a = \frac{1 + 2\xi - 12\xi(1-\xi)\lambda}{(1-\xi)^2} \tag{A9}$$

$$b = \frac{-3\xi + 12\xi(1-\xi)\lambda}{2(1-\xi)^2} \tag{A10}$$

This value for a inserted in Eq. (A2) via (A7) gives Eq. (8) with λ related to λ_1 by Eq. (A5).

Utilizing Eq. (A7) in (A6) we finally get

$$1 + h(1^+) = a + b + 12\xi\lambda Q(0)$$

$$= a + b + 12\xi\lambda(-\frac{1}{2}a - b + \lambda)$$

$$= \frac{1 + \xi/2}{(1-\xi)^2} - \frac{12\xi\lambda}{1-\xi} + 12\xi\lambda^2 \tag{A11}$$

which using Eq.(2) and the continuity of $y(r)$ at the core yield the sought Eq.(7).

[1] J.S. Høye, E. Lomba and G. Stell, Mol. Phys., **75**, 1217 (1992)

[2] L. Belloni, J. Chem. Phys., submitted

[3] M. Kinoshita and M. Harada, Mol. Phys., **65**, 599 (1988); *ibidem*, **70**, 1121 (1990)

[4] R.J. Baxter, J. chem. Phys., **49**, 2770 (1968)

[5] P.T. Cummings and G. Stell, J. chem. Phys., **78**, 1917 (1983) and references therein.

[6] E. Waisman, Mol. Phys., **25**, 45 (1973)

[7] J.S. Høye and G. Stell, Mol. Phys., **32**, 195 (1976); *ibid.* **32**, 209 (1976)

[8] J.S.Høye and L. Blum, J. stat. Phys, **16**, 399 (1977)

[9] J.S. Høye and G. Stell, J. chem. Phys., **73**, 461 (1980)

[10] J.S. Høye and E. Lomba, J. chem. Phys., **93**, 4272 (1990)

[11] F. Gallerani, G. Lo Vecchio and L. Reatto, Phys. Rev. A, **32**, 2526 (1985)

[12] F. Gallerani, G. Lo Vecchio and L. Reatto, Phys. Rev. A, **31**, 511 (1985)

[13] A. Parola and L. Reatto, Physica A, **125**, 255 (1984)

[14] E. Lomba, Mol. Phys., **68**, 87 (1989)

[15] P.D. Poll and N.W. Ashcroft, Phys. Rev. A. **32** 1722 (1985)

[16] J. Hafner and W. Jank, Z. Phys. B-Condensed Matter, **70**, 81 (1988)

[17] P.E. Gill, W. Murray and M.H. Wright, *Practical Optimization*, (Academic, New York, 1981)

[18] M.S. Green, J. chem. Phys., **33**, 1403 (1960)

[19] G. Stell, J.L. Lebowitz, S. Baer and W. Theumann, J. Math. Phys, **7**, 15332 (1966)

[20] G. Stell, Phys. Rev. A, **45**, 7628 (1992)

FIGURES

FIG. 1. No-solution region for the HNC equation (delineated by solid lines obtained from numerical solution) for the pure RPM and for shielded RPM ($z = 1$ and $z = 2$) compared with low density theoretical estimate (dotted lines) given by Eq. (19) and Eq. (21).

FIG. 2. Isothermal compressibility *vs* T^* for Lennard-Jones and RPM fluids in the HNC approximation in the vicinitiy of the no solution locus. Solid lines denote a a non linear fit to Eq.(22) and points are integral equation results

FIG. 3. Density dependence of the b parameter in Eq. (22) for Lennard-Jones and RPM fluids in the HNC approximation. Lines connecting points are drawn as a guide
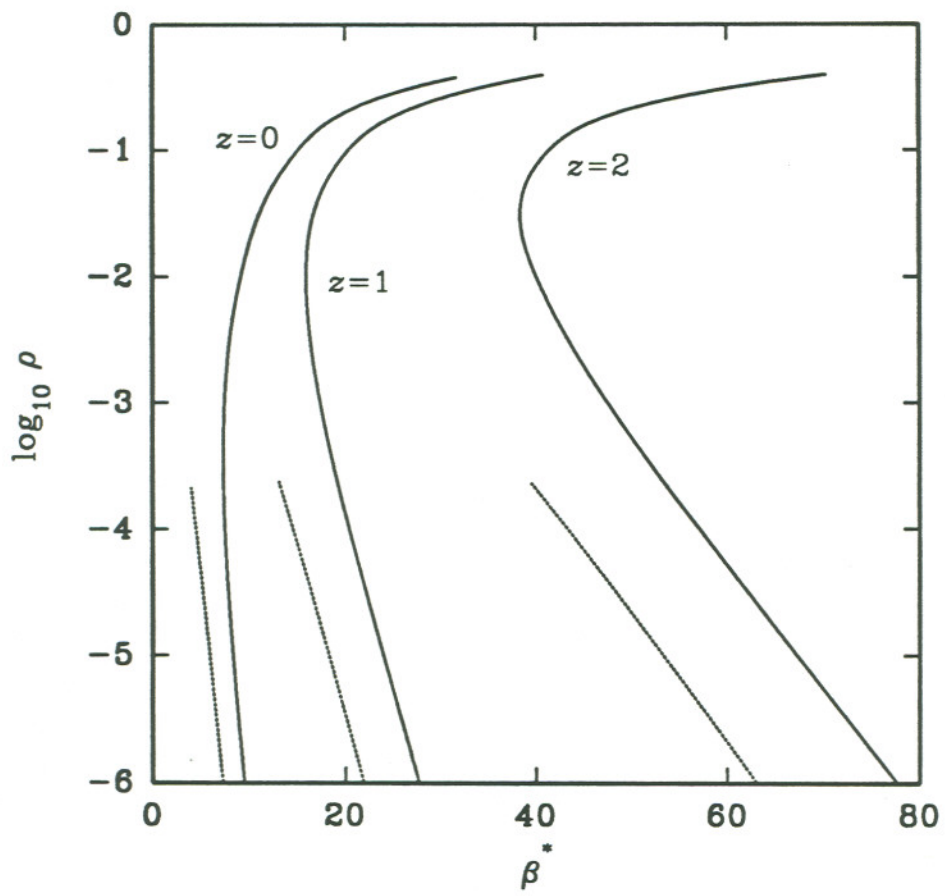
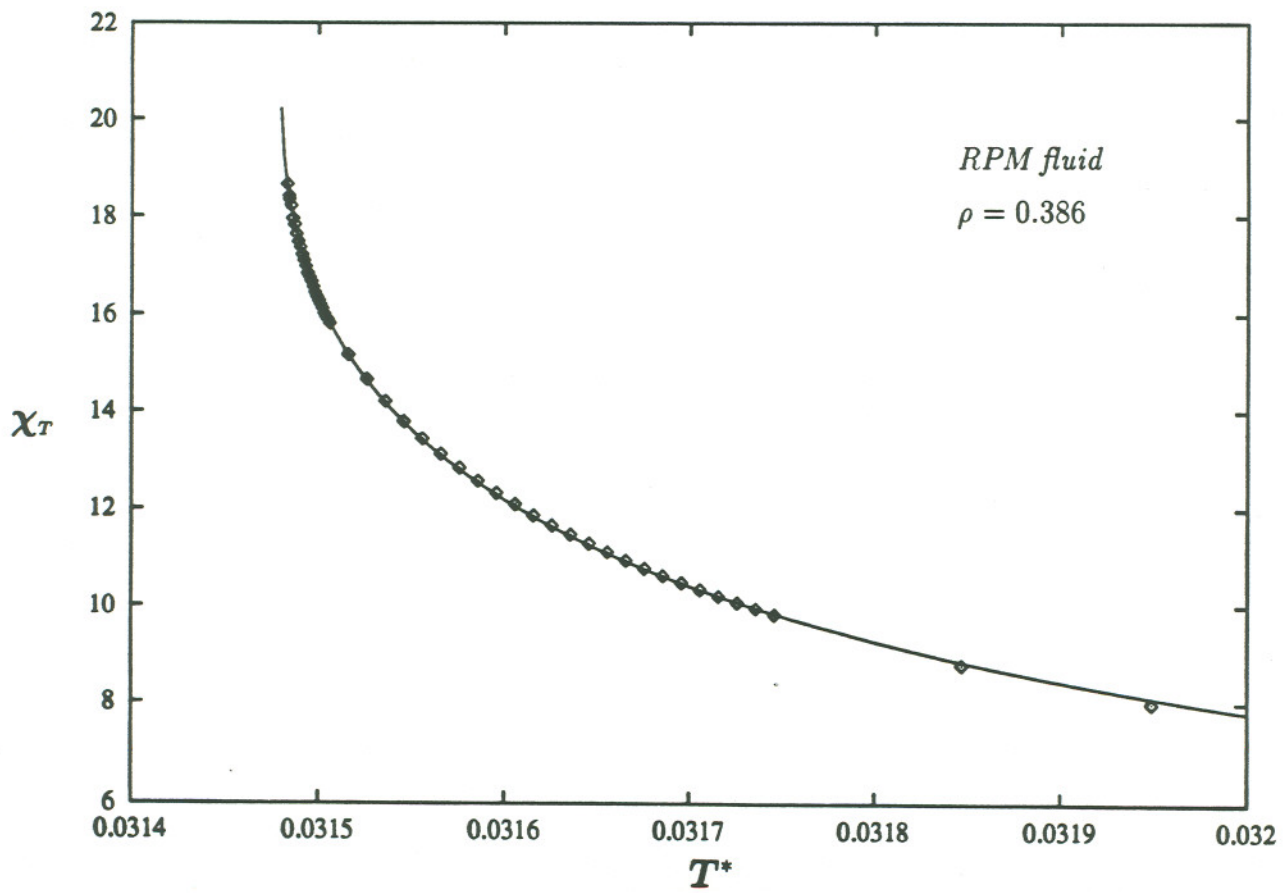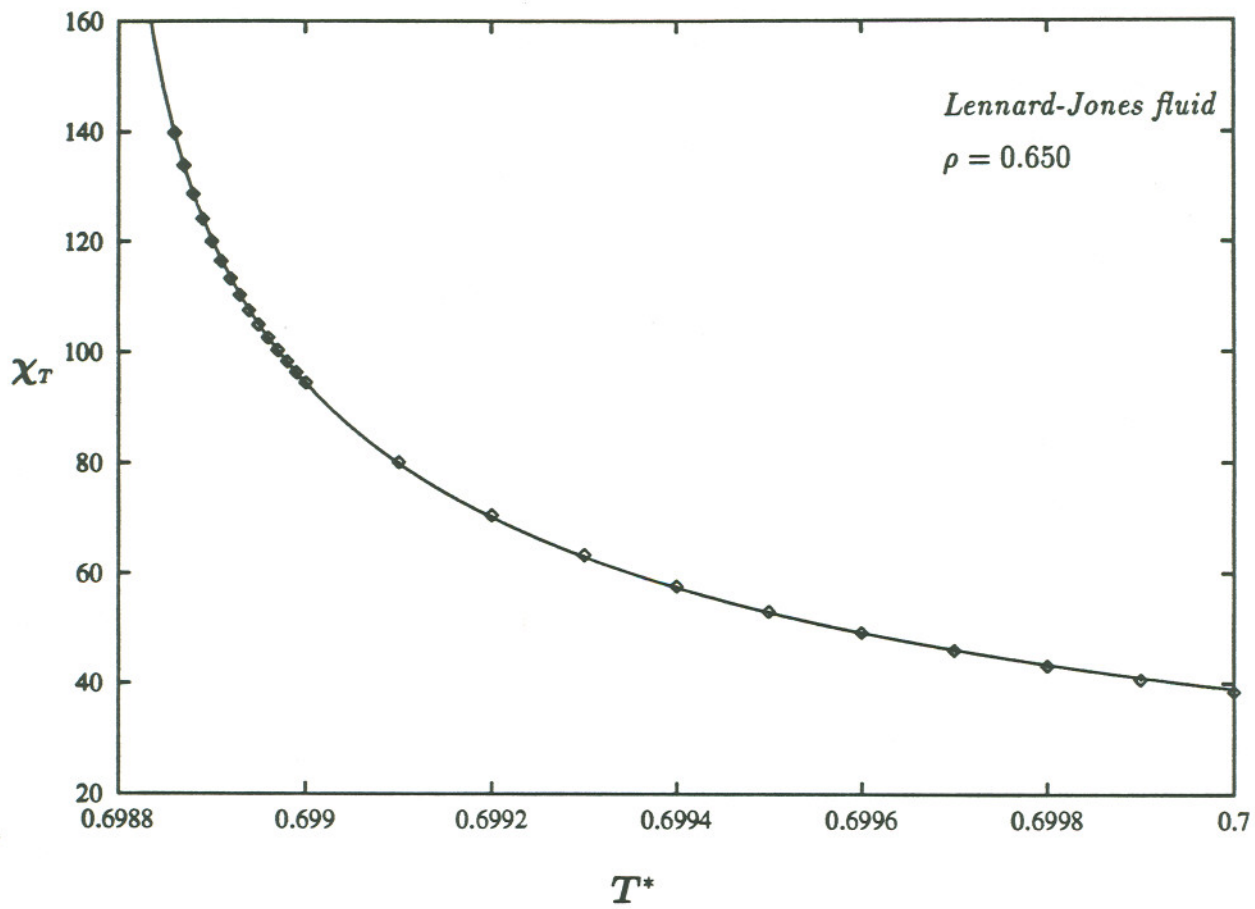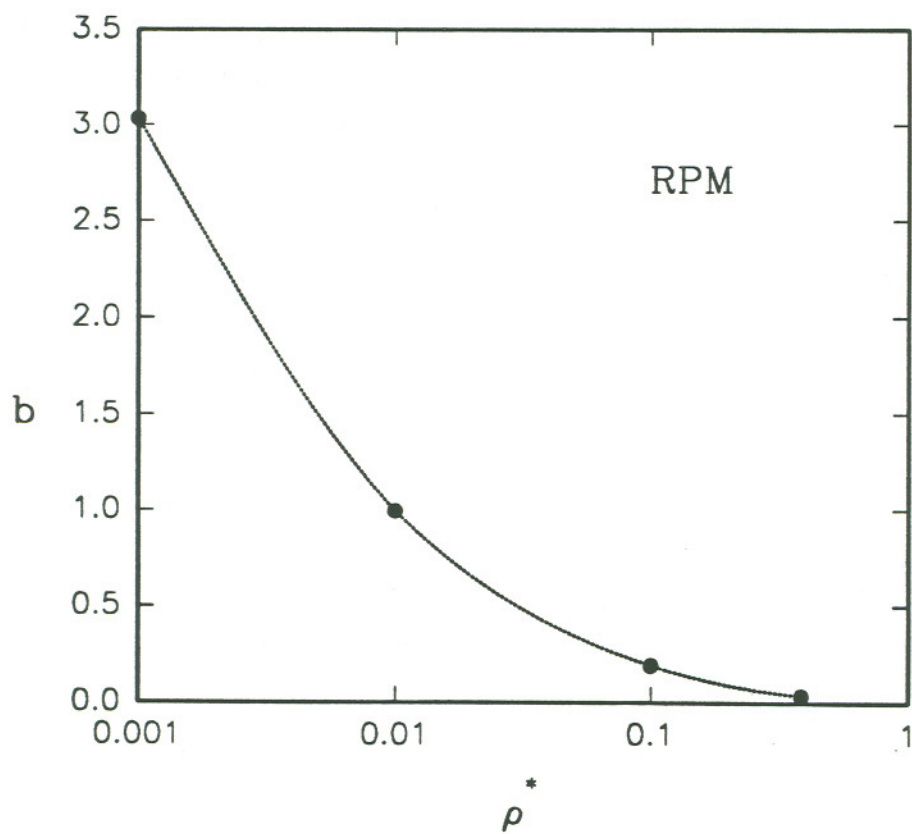**Figure 1.** J.S. Høye *et al.*, Analysis of the hypernetted chain equation

Figure 2. J.S. Høye *et al.*, Analysis of the hypernetted chain equation
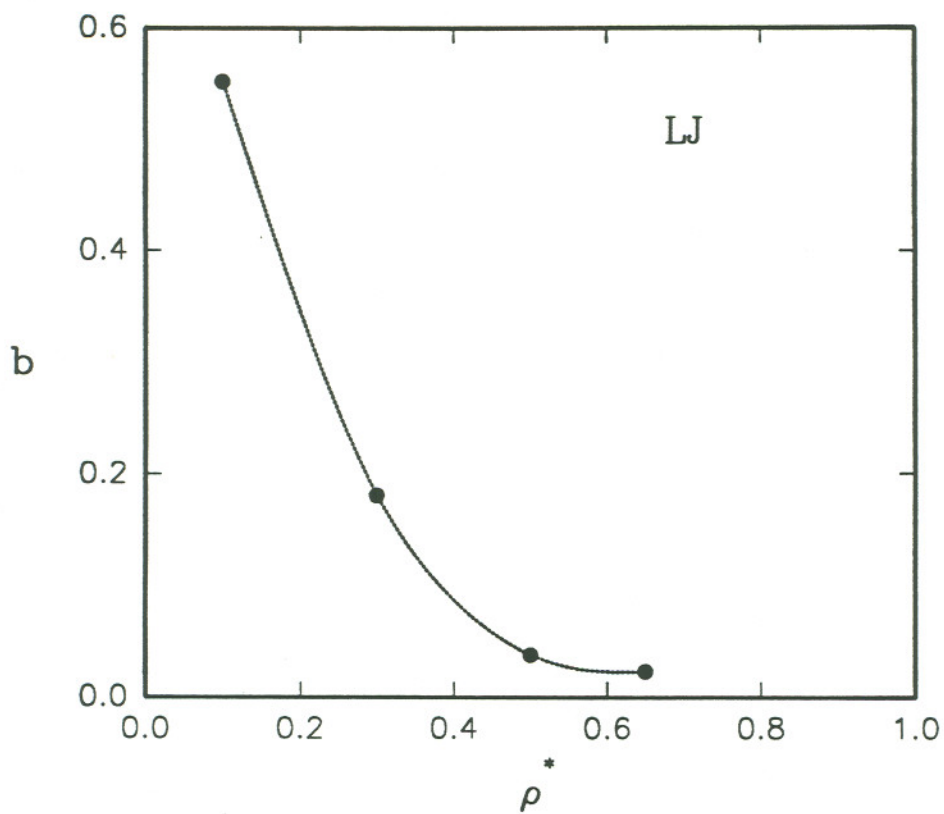
Figure 3. J.S. Høye *et al.*, Analysis of the hypernetted chain equation